Minimax Design of 2-D Complex-Coefficient FIR Filters with Low Group Delay using Semidefinite Programming

Ashira L. Jayaweera*, Sakila S. Jayaweera*, Chamira U. S. Edussooriya*, Chamith Wijenayake†, and Arjuna Madanayake‡
*Department of Electronic and Telecommunication Engineering, University of Moratuwa, Moratuwa, Sri Lanka
†School of Information Technology and Electrical Engineering, University of Queensland, Brisbane, QLD, Australia
‡Department of Electrical and Computer Engineering, Florida International University, Miami, FL, USA
Emails: {ashiraj,sakilaj,chamira}@uom.lk, c.wijenayake@uq.edu.au, amadanay@fiu.edu

***Abstract*—A minimax design for 2-D complex-coefficient FIR filters having asymmetric frequency responses is proposed in this paper. We consider the general form of 2-D FIR filters with low group delay and formulate the minimax design as a semidefinite programming problem. The 2-D linear-phase FIR filters with conjugate-symmetric coefficients are a special case of the proposed design. Example filter designs having near-equiripple magnitude responses are presented to verify the effectiveness of the proposed design method.**

***Index Terms*—2-D FIR filters, complex-coefficient, minimax design, equiripple, semidefinite programming.**

I. Introduction

Two-dimensional (2-D) filters are employed in numerous applications in image processing and array signal processing [1]–[10], and in designing higher-dimensional filters [11]–[17]. Two-dimensional finite-extent impulse response (FIR) filters are often preferred to 2-D infinite-extent impulse response (IIR) filters in many applications because the former are inherently stable and can be designed to have constant group delay despite having higher computational complexities compared to the latter. Two-dimensional FIR filters can be designed using the windowing technique, the McClellan transform or optimization techniques [1, chs. 6 and 9], [2, ch .4], [3, ch. 3], [18]. These techniques predominantly consider the design of 2-D FIR filters having symmetric frequency responses of which the underlying filter coefficients are real-valued. A number of optimization techniques have been developed in the last three decades; see [19]–[31] and the references therein. In particular, a semidefinite programming approach is presented in [32] for both 2-D real-coefficient FIR and IIR filters.

Two-dimensional FIR filters having *asymmetric* frequency responses, hence having complex-valued coefficients, are required in applications such as wideband receive-mode beamforming with down-converted radio-frequency signals encountered in antenna arrays [33]–[36] and complex wavelet transform [37]–[40]. Despite the least-square design approach proposed in [41] and the windowing-technique based designs proposed in [33]–[36], very little work has been done towards to design of 2-D complex-coefficient FIR filters.

In this paper, a minimax design for 2-D complex-coefficient FIR filters having asymmetric frequency responses is proposed. We consider the general form of 2-D FIR filters with low group delay, where coefficients do not posses the conjugate symmetry. The class of 2-D linear-phase FIR filters with conjugate-symmetric coefficients are a special case of the proposed method. The minimax design is formulated as a semidefinite program, which can be efficiently solved using SeDuMi [42] or CVX [43], [44] optimization toolboxes. To the best of authors' knowledge, the proposed method is the first minimax design method developed to design 2-D complex-coefficient FIR filters with low group delay. Example filter designs, with near-equiripple passband and stopband magnitude responses, are presented to verify the effectiveness of the proposed method.

II. Proposed Minimax Design Method

A. Problem Formulation

In this subsection, we present the formulation of the minimax design of 2-D complex-coefficient FIR filters with low group delay. To this end, we consider a 2-D FIR filter of order $(N_1-1)\times(N_2-1)$ of which the transfer function is given by

$$H(z_1,z_2)=\sum_{n_1=0}^{N_1-1}\sum_{n_2=0}^{N_2-1}h(n_1,n_2)z_1^{-n_1}z_2^{-n_2}, \qquad (1)$$

where $h(n_1,n_2)$ is the complex-valued impulse response. The frequency response of $H(z_1,z_2)$ can be obtained by evaluating $H(z_1,z_2)$ on the unit bi-circle as

$$\begin{aligned}H(e^{j\omega_1},e^{j\omega_2})&=\sum_{n_1=0}^{N_1-1}\sum_{n_2=0}^{N_2-1}h(n_1,n_2)e^{-j(\omega_1 n_1+\omega_2 n_2)}\\&=\boldsymbol{e_1}^{\mathrm{T}}\boldsymbol{H}\boldsymbol{e_2}, \qquad (2)\end{aligned}$$

978-1-7281-3320-1/20/$31.00 ©2020 IEEE

where

$$\boldsymbol{H} = \begin{bmatrix} h(0,0) & h(0,1) & \cdots & h(0,N_2-1) \\ h(1,0) & h(1,1) & \cdots & h(1,N_2-1) \\ \vdots & \vdots & \ddots & \vdots \\ h(N_1-1,0) & h(N_1-1,1) & \cdots & h(N_1-1,N_2-1) \end{bmatrix}$$

$$\boldsymbol{e_1} = \begin{bmatrix} 1 & e^{-j\omega_1} & e^{-j2\omega_1} & \cdots & e^{-j(N_1-1)\omega_1} \end{bmatrix}^{\mathrm{T}}$$
$$\boldsymbol{e_2} = \begin{bmatrix} 1 & e^{-j\omega_2} & e^{-j2\omega_2} & \cdots & e^{-j(N_2-1)\omega_2} \end{bmatrix}^{\mathrm{T}}.$$

Here, $H(e^{j\omega_1}, e^{j\omega_2})$ is considered only for the principal Nyquist square $\mathcal{N}$ $(= \{(\omega_1, \omega_2) \in \mathbb{R}^2 \mid -\pi \le \omega_1, \omega_2 < \pi\})$. The expression in (2) can be expanded as

$$\begin{aligned} H(e^{j\omega_1}, e^{j\omega_2}) &= [\boldsymbol{c_1}(\omega_1) - j\boldsymbol{s_1}(\omega_1)]^{\mathrm{T}}\boldsymbol{H}[\boldsymbol{c_2}(\omega_2) - j\boldsymbol{s_2}(\omega_2)] \\ &= \mathrm{trace}[\boldsymbol{P}(\omega_1,\omega_2)\boldsymbol{H}] \\ &\quad - j(\mathrm{trace}[\boldsymbol{Q}(\omega_1,\omega_2)\boldsymbol{H}]), \end{aligned} \tag{3}$$

where

$$\boldsymbol{c_i}(\omega_i) = \begin{bmatrix} 1 & \cos(\omega_i) & \cos(2\omega_i) & \cdots & \cos((N_i-1)\omega_i) \end{bmatrix}^{\mathrm{T}}$$
$$\boldsymbol{s_i}(\omega_i) = \begin{bmatrix} 0 & \sin(\omega_i) & \sin(2\omega_i) & \cdots & \sin((N_i-1)\omega_i) \end{bmatrix}^{\mathrm{T}}$$
$$\boldsymbol{P}(\omega_1,\omega_2) = \boldsymbol{c_2}(\omega_2)\boldsymbol{c_1}(\omega_1)^{\mathrm{T}} - \boldsymbol{s_2}(\omega_2)\boldsymbol{s_1}(\omega_1)^{\mathrm{T}}$$
$$\boldsymbol{Q}(\omega_1,\omega_2) = \boldsymbol{c_2}(\omega_2)\boldsymbol{s_1}(\omega_1)^{\mathrm{T}} + \boldsymbol{s_2}(\omega_2)\boldsymbol{c_1}(\omega_1)^{\mathrm{T}},$$

where $i = 1, 2$. Now, we create the column vectors $\boldsymbol{p}(\omega_1, \omega_2)$ and $\boldsymbol{q}(\omega_1, \omega_2)$ by stacking transposed rows of $\boldsymbol{P}(\omega_1, \omega_2)$ and $\boldsymbol{Q}(\omega_1, \omega_2)$, respectively, and a column vector $\boldsymbol{h}$ by stacking columns of $\boldsymbol{H}$. Next, $H(e^{j\omega_1}, e^{j\omega_2})$ can be expressed as

$$H(e^{j\omega_1}, e^{j\omega_2}) = \boldsymbol{p}^{\mathrm{T}}(\omega_1,\omega_2)\boldsymbol{h} - j\boldsymbol{q}^{\mathrm{T}}(\omega_1,\omega_2)\boldsymbol{h}. \tag{4}$$

Furthermore, we express the complex-valued impulse response as $\boldsymbol{h} = \boldsymbol{h}_r + j\boldsymbol{h}_i$, where $\boldsymbol{h}_r$ and $\boldsymbol{h}_i$ are the real and imaginary parts of $\boldsymbol{h}$, respectively. Then, the frequency response can be formulated as,

$$\begin{aligned} H(e^{j\omega_1}, e^{j\omega_2}) &= \boldsymbol{p}^{\mathrm{T}}(\omega_1,\omega_2)(\boldsymbol{h}_r + j\boldsymbol{h}_i) \\ &\quad - j\boldsymbol{q}^{\mathrm{T}}(\omega_1,\omega_2)(\boldsymbol{h}_r + j\boldsymbol{h}_i) \\ &= \boldsymbol{p}^{\mathrm{T}}(\omega_1,\omega_2)\boldsymbol{h}_r + \boldsymbol{q}^{\mathrm{T}}(\omega_1,\omega_2)\boldsymbol{h}_i \\ &\quad - j\begin{bmatrix} \boldsymbol{q}^{\mathrm{T}}(\omega_1,\omega_2) & -\boldsymbol{p}^{\mathrm{T}}(\omega_1,\omega_2) \end{bmatrix} \begin{bmatrix} \boldsymbol{h}_r \\ \boldsymbol{h}_i \end{bmatrix} \\ &= \boldsymbol{a}^{\mathrm{T}}(\omega_1,\omega_2)\boldsymbol{h}_c - j\boldsymbol{b}^{\mathrm{T}}(\omega_1,\omega_2)\boldsymbol{h}_c, \end{aligned} \tag{5}$$

where $\boldsymbol{a}(\omega_1,\omega_2) = \begin{bmatrix} \boldsymbol{p}^{\mathrm{T}}(\omega_1,\omega_2) & \boldsymbol{q}^{\mathrm{T}}(\omega_1,\omega_2) \end{bmatrix}^{\mathrm{T}}$, $\boldsymbol{b}(\omega_1,\omega_2) = \begin{bmatrix} \boldsymbol{q}^{\mathrm{T}}(\omega_1,\omega_2) & -\boldsymbol{p}^{\mathrm{T}}(\omega_1,\omega_2) \end{bmatrix}^{\mathrm{T}}$, and $\boldsymbol{h}_c = \begin{bmatrix} \boldsymbol{h}_r & \boldsymbol{h}_i \end{bmatrix}^{\mathrm{T}}$.

Now the minimax design of the 2-D complex-coefficient FIR filter can be expressed as the minimization problem given by

$$\underset{\boldsymbol{h}_c}{\text{minimize}} \ \|J(\boldsymbol{h}_c, \omega_1, \omega_2)\|_\infty, \tag{6}$$

where $\|\cdot\|_\infty$ is the infinity-norm of a vector, and the objective function $J(\boldsymbol{h}_c, \omega_1, \omega_2)$ is defined as

$$\begin{aligned} J(\boldsymbol{h}_c, \omega_1, \omega_2) = W(\omega_1,\omega_2)\,&[H(e^{j\omega_1}, e^{j\omega_2}) \\ &-H_d(e^{j\omega_1}, e^{j\omega_2})]\,. \end{aligned} \tag{7}$$

Here, $H_d(e^{j\omega_1}, e^{j\omega_2})$ is the ideal frequency response of the required filter, and $W(\omega_1, \omega_2)$ is a nonnegative weighting function. Note that the ideal frequency response $H_d(e^{j\omega_1}, e^{j\omega_2})$ can be expressed as

$$H_d(e^{j\omega_1}, e^{j\omega_2}) = M_d(\omega_1,\omega_2)e^{-j(d_1\omega_1 + d_2\omega_2)}, \tag{8}$$

where $M_d(\omega_1, \omega_2)$ is the desired magnitude response and d_1 $(0 < d_1 \le (N_1-1)/2)$ and d_2 $(0 < d_2 \le (N_2-1)/2)$ are the constant group delays with respect to ω_1 and ω_2, respectively.

B. Semidefinite Programming Approach

We convert the optimization problem in (6) to a semidefinite programming problem in this subsection. To this end, we consider the equivalent optimization problem to that in (6) given by

$$\underset{\boldsymbol{h}_c}{\text{minimize}} \quad \beta \tag{9a}$$

$$\text{subject to} \quad \|J(\boldsymbol{h}_c, \omega_1, \omega_2)\|_\infty^2 \le \ \beta \ \text{ for } (\omega_1, \omega_2) \in \mathcal{N} \tag{9b}$$

following an approach similar to those employed for one-dimensional and 2-D real-coefficient FIR filters designs [32], [45, ch. 16.2], where β is an upper bound on $\|J(\boldsymbol{h}_c, \omega_1, \omega_2)\|_\infty^2$. The function $\|J(\boldsymbol{h}_c, \omega_1, \omega_2)\|_\infty^2$ can be expressed using (5) and (8) as

$$\begin{aligned} \|J(\boldsymbol{h}_c, \omega_1, \omega_2)\|_\infty^2 &= W^2(\omega_1,\omega_2)|H(e^{j\omega_1}, e^{j\omega_2}) \\ &\qquad - H_d(e^{j\omega_1}, e^{j\omega_2})|^2 \\ &= W^2(\omega_1,\omega_2)\Big[\big(\boldsymbol{a}^{\mathrm{T}}(\omega_1,\omega_2)\boldsymbol{h}_c - H_{dr}(\omega_1,\omega_2)\big)^2 \\ &\quad + \big[\boldsymbol{b}^{\mathrm{T}}(\omega_1,\omega_2)\boldsymbol{h}_c - H_{di}(\omega_1,\omega_2)\big)^2\Big] \\ &= \alpha_1^2(\omega_1,\omega_2) + \alpha_2^2(\omega_1,\omega_2), \end{aligned} \tag{10}$$

where

$$\alpha_1(\omega_1,\omega_2) = \boldsymbol{a_w}^{\mathrm{T}}(\omega_1,\omega_2)\boldsymbol{h}_c - \hat{H}_{dr}(\omega_1,\omega_2)$$
$$\alpha_1(\omega_1,\omega_2) = \boldsymbol{b_w}^{\mathrm{T}}(\omega_1,\omega_2)\boldsymbol{h}_c - \hat{H}_{di}(\omega_1,\omega_2),$$

and

$$\boldsymbol{a_w}(\omega_1,\omega_2) = W(\omega_1,\omega_2)\boldsymbol{a}(\omega_1,\omega_2)$$
$$\boldsymbol{b_w}(\omega_1,\omega_2) = W(\omega_1,\omega_2)\boldsymbol{b}(\omega_1,\omega_2)$$
$$\widehat{H}_{dr}(\omega_1,\omega_2) = W(\omega_1,\omega_2)H_{dr}(\omega_1,\omega_2)$$
$$\widehat{H}_{di}(\omega_1,\omega_2) = W(\omega_1,\omega_2)H_{di}(\omega_1,\omega_2).$$

Note that

$$H_{dr}(\omega_1,\omega_2) = M_d(\omega_1,\omega_2)\cos(d_1\omega_1 + d_2\omega_2)$$
$$H_{di}(\omega_1,\omega_2) = M_d(\omega_1,\omega_2)\sin(d_1\omega_1 + d_2\omega_2).$$

Using (10), the constraint in (9b) can be expressed as

$$\beta - \alpha_1^2(\omega_1,\omega_2) - \alpha_2^2(\omega_1,\omega_2) \ge 0 \ \text{ for } (\omega_1,\omega_2) \in \mathcal{N} \tag{11}$$

and it can be shown that this inequality holds if and only if the matrix $\boldsymbol{D}(\omega_1, \omega_2)$ defined as

$$\boldsymbol{D}(\omega_1,\omega_2) = \begin{bmatrix} \beta & \alpha_1(\omega_1,\omega_2) & \alpha_2(\omega_1,\omega_2) \\ \alpha_1(\omega_1,\omega_2) & 1 & 0 \\ \alpha_2(\omega_1,\omega_2) & 0 & 1 \end{bmatrix} \tag{12}$$

is positive semidefinite for $(\omega_1, \omega_2) \in \mathcal{N}$ [45, ch. 16.2]. Next, we define $\boldsymbol{x} = \begin{bmatrix}\beta & \boldsymbol{h}_c^{\mathrm{T}}\end{bmatrix}^{\mathrm{T}}$, which is a $(2N_1N_2 + 1)$-dimensional vector, and $\boldsymbol{D}(\omega_1, \omega_2)$ is affine with respect to x [32], [45, ch. 16.2]. Then, we consider the discretized version of the constraint $\boldsymbol{D}(\omega_1, \omega_2) \succcurlyeq 0$ with a dense set of frequencies $\mathcal{N}_d = \{(\omega_1^k, \omega_2^k) \mid k = 1, 2, \ldots K\} \subseteq \mathcal{N}$. In this case, $\boldsymbol{D}(\omega_1, \omega_2) \succcurlyeq 0$ becomes

$$\boldsymbol{F}(\boldsymbol{x}) \succcurlyeq 0 \tag{13}$$

where,

$$\boldsymbol{F}(\boldsymbol{x}) = \mathrm{diag}\left\{\boldsymbol{D}(\omega_1^1, \omega_2^1), \boldsymbol{D}(\omega_1^2, \omega_2^2), \cdots, \boldsymbol{D}(\omega_1^K, \omega_2^K)\right\}. \tag{14}$$

Using (14), the optimization problem in (9) can be formulated to a semidefinite programming problem [45, ch. 14.2] as

$$\text{minimize} \quad \boldsymbol{f}^{\mathrm{T}}\boldsymbol{x} \tag{15a}$$
$$\text{subject to} \quad \boldsymbol{F}(\boldsymbol{x}) \succcurlyeq 0 \tag{15b}$$

where $\boldsymbol{f} = \begin{bmatrix}1 & 0 & 0 & \cdots & 0\end{bmatrix}^{\mathrm{T}}_{1\times(2N_1N_2+1)}$.

III. Design Examples

In this section, we present design examples of a 2-D circular filter and a 2-D trapezoidal filter in order to confirm the effectiveness of the proposed method. For both filter designs, we employ CVX [43], [44] as the optimization toolbox with an Intel Core i7-4770 processor (3.4 GHz) and 16 GB RAM.

A. Example I

In the first example, we consider the design of a 2-D FIR shifted circularly-symmetric filter with low group delay. Such filters are required for beamforming of narrowband radio-frequency plane waves received by uniform planar arrays [46, ch. 4]. The specifications of the magnitude response of the filter is selected as same as the second example presented in [41], i.e., the passband is a circle of which the center is $(-0.3\pi, 0.2\pi)$ rad/sample and the radius is 0.3π rad/sample; the stopband is the outside region of a circle having the same center and a radius of 0.5π rad/s. However, we consider a lower group delay filter whereas the weighted-least square design in [41] is a linear-phase filter. The 2-D filter is designed with orders of 10×10, 16×16, 22×22, and 28×28, with the group delays of $(4,4)$, $(6,6)$, $(8,8)$ and $(10,10)$, respectively. The weight function $W(\omega_1, \omega_2)$ is selected to obtain near equiripple magnitude responses, with $W(\omega_1, \omega_2) = 0$ for the transition band. For example, for the filter having order 28×28, the $W(\omega_1, \omega_2)$ is selected as

$$W(\omega_1, \omega_2) = \begin{cases} 1, & (\omega_1, \omega_2) \in \text{passband} \\ 0, & (\omega_1, \omega_2) \in \text{transition band} \\ 1, & \{(\omega_1, \omega_2) \in \text{stopband}\} \cap \\ & \{-0.75\pi \le \omega_1 \le 0.15\pi \\ & \qquad \cup -0.25\pi \le \omega_2 \le 0.65\pi\} \\ 0.05, & \text{otherwise.} \end{cases}$$

Furthermore, 60×60, 70×70, 70×70, and 80×80 point grids are selected, respectively, and the number of grid points in the passband and the stopband regions are 3277, 4429, 4429 and 5757, respectively. The maximum passband ripple δ_p and the minimum stopband attenuation δ_s achieved with each filter, and the maximum absolute errors $e_{d,1}$ and $e_{d,2}$ of the group delays are presented in Table I. The filter designs take 49.17 s, 173.72 s, 495.67 s, and 1970.97 s, respectively. The magnitude response and the group delay in the passband with respect to ω_1 and ω_2 of the filter having the order 28×28 are shown in Figs. 1(a), 1(b) and 1(c), respectively. It can be observed that the magnitude response is near equiripple. Furthermore, according to Table I, with the filter of order 28×28, 0.025 dB passband ripple and 50 dB stopband attenuation can be achieved with less than 3% deviation of the group delay. These results confirm the effectiveness of the proposed minimax design method. Note that, to the best of our knowledge, we are unaware of previously reported minimax design methods for 2-D FIR complex-coefficient filters with low group delay in order to perform a fair comparison.

TABLE I: The maximum passband ripple, the minimum stopband attenuation, and the maximum absolute errors of the group delays of the designed 2-D FIR shifted circularly-symmetric filter.

Filter order	10×10	16×16	22×22	28×28
δ_p (dB)	0.4790	0.1573	0.0648	0.0250
δ_s (dB)	25.3371	33.7812	42.5545	50.7942
$e_{d,1}$	0.3174	0.4623	0.4293	0.2851
$e_{d,2}$	0.3174	0.4944	0.3783	0.2851

B. Example II

In the second example, we consider the design of a 2-D linear-phase FIR trapezoidal filter typically employed for wideband beamforming of radio-frequency plane waves received by uniform linear arrays at the baseband [33]–[36]. The magnitude response of such a filter is specified by the angles θ_1 and θ_2, the cutoff frequencies $\omega_{1,cl}$, $\omega_{1,cu}$ and $\omega_{2,c}$, and the width of the transition band ω_t as shown in Fig 2. The 2-D trapezoidal filter is designed for the specifications $\theta_1 = 89.3°$, $\theta_2 = 88.7°$, $\omega_{1,cl} = 0.24\pi$ rad/sample, $\omega_{1,cu} = 0.43\pi$ rad/sample, $\omega_{2,c} = 0.83\pi$ rad/sample and $\omega_t = 0.1\pi$ rad/sample, with orders of 10×10, 16×16, 22×22, and 28×28. Due to the linear-phase responses, the constant group delays of the filters are $(5,5)$, $(8,8)$, $(11,11)$ and $(14,14)$, respectively. The weight function $W(\omega_1, \omega_2)$ is selected as $W(\omega_1, \omega_2) = 1$ for both passband and stopband, and $W(\omega_1, \omega_2) = 0$ for the transition band leading to equiripple magnitude responses. Similar to the design example I, 60×60, 70×70, 70×70, and 80×80 point grids are selected, respectively, and the number of grid points in the passband and the stopband regions are 3355, 4541, 4541 and 5901, respectively. The maximum passband ripple δ_p and the minimum stopband attenuation δ_s achieved with each example design are presented in Table II. The filter designs take 51.31 s, 329.79 s, 844.71 s, and 2739.51 s, respectively. The magnitude response of the filter of order 28×28 is shown in Fig. 3. It can be observed that the

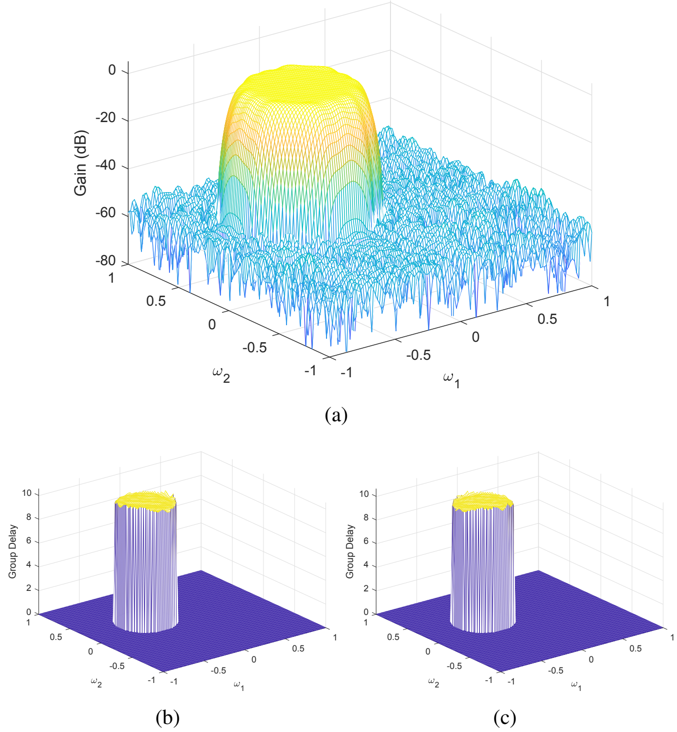

Fig. 1: (a) The magnitude response and the group delay, (b) with respect to ω_1 and (c) with respect to ω_2, of the 2-D FIR shifted circularly-symmetric filter having the order 28×28 in the passband.

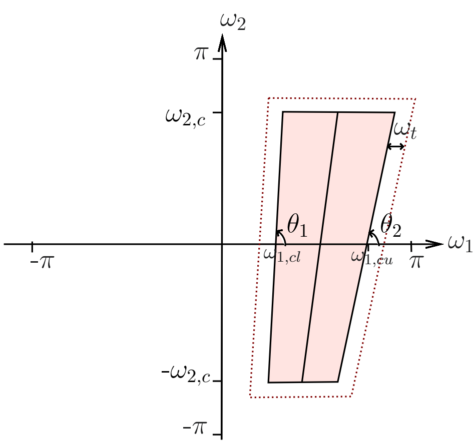

Fig. 2: The ideal passband of a 2-D trapezoidal filter.

magnitude response is near equiripple. Furthermore, all the filters achieved more than 15 dB stopband attenuation. In particular, a stopband attenuation of 30 dB and a maximum passband ripple of 0.03 dB are achieved with the filter of order 28×28.

Two-dimensional linear-phase FIR trapezoidal filters having the same orders and similar passbands are designed using the windowing technique with 2-D separable Dolph-Chebyshev windows [36]. Note that the Dolph-Chebyshev window leads to near equiripple passband and stopband magnitude responses [47, ch. 9.3]. The ripple-ratio parameter of the

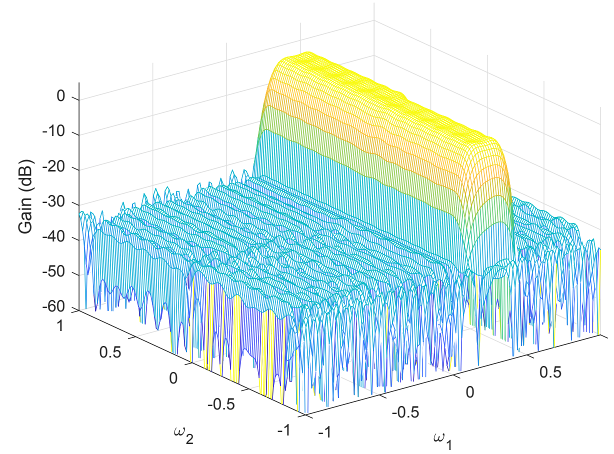

Fig. 3: The magnitude response of the 2-D FIR trapezoidal filter of order 28×28.

TABLE II: The maximum passband ripple and the minimum stopband attenuation of the designed 2-D linear-phase FIR trapezoidal filters.

Filter order	10×10	16×16	22×22	28×28
proposed method				
δ_p (dB)	0.1707	0.1131	0.0604	0.0305
δ_s (dB)	15.3570	18.9312	24.3844	30.3189
method in [36]				
δ_p (dB)	3.2811	2.8608	1.5625	0.5995
δ_s (dB)	15.2860	18.9100	24.1368	30.1992

Dolph-Chebyshev windows are selected to achieve minimum stopband attenuations (δ_s) similar to those obtained with the proposed filter design method. The maximum passband ripple δ_p and the minimum stopband attenuation δ_s achieved with each filter are presented in Table II. It is evident that the proposed minimax design method provides significantly small passband ripple compared to those achieved with the filters designed using the windowing technique [36] for similar minimum stopband attenuations. These results confirm the effectiveness of the proposed minimax design method.

IV. Conclusions and Future Work

A minimax design for 2-D complex-coefficient FIR filters having asymmetric frequency responses and low group delay is proposed. The minimax design is formulated as a semidefinite programming problem. Two design examples are presented to confirm the effectiveness of the proposed method. In particular, near-equiripple magnitude responses with small passband ripple can be achieved with the proposed minimax design method. Future work includes the extension of the proposed method to design 2-D sparse complex-coefficient FIR filters and discrete-space continuous-time 2-D complex-coefficient FIR filters for beamforming applications.

Acknowledgment

The authors thank Prof. Wu-Sheng Lu, University of Victoria, Victoria, BC, Canada for insightful comments.

REFERENCES

[1] W.-S. Lu and A. Antoniou, *Two-Dimensional Digital Filters*. NY: Marcel Dekker, 1992.

[2] J. S. Lim, *Two-Dimensional Signal and Image Processing*. Upper Saddle River, NJ: Prentice-Hall, 1990.

[3] D. E. Dudgeon and R. M. Mersereau, *Multidimensional Digital Signal Processing*. Englewood Cliffs, NJ: Prentice-Hall, 1984.

[4] S. Haykin, *Array Signal Processing*. Englewood Cliffs, NJ: Prentice-Hall, 1985.

[5] T. Sekiguchi and Y. Karasawa, "Wideband beamspace adaptive array utilizing FIR fan filters for multibeam forming," *IEEE Trans. Signal Process.*, vol. 48, no. 1, pp. 277–284, Jan. 2000.

[6] K. Nishikawa, "Wideband multi-beam forming method using delayed array sensors and two-dimensional digital filter," *Electron. and Commun. in Japan, Part 3*, vol. 88, no. 12, pp. 1–12, Dec. 2005.

[7] T. K. Gunaratne and L. T. Bruton, "Beamforming of broad-band bandpass plane waves using polyphase 2-D FIR trapezoidal filters," *IEEE Trans. Circuits Syst. I*, vol. 55, no. 3, pp. 838–850, Apr. 2008.

[8] C. Wijenayake, A. Madanayake, Y. Xu, L. Belostotski, and L. T. Bruton, "A steerable DC-1 GHz all-pass filter-sum RF space-time 2-D beam filter in 65 nm CMOS," in *Proc. IEEE Int. Symp. Circuits Syst.*, 2013, pp. 1276–1279.

[9] C. Wijenayake, A. Madanayake, L. T. Bruton, and V. Devabhaktuni, "DOA-estimation and source-localization in CR-networks using steerable 2-D IIR beam filters," in *Proc. IEEE Int. Symp. Circuits Syst.*, 2013, pp. 65–68.

[10] C. Wijenayake, A. Madanayake, L. Belostotski, Y. Xu, and L. Bruton, "All-pass filter-based 2-D IIR filter-enhanced beamformers for AESA receivers," *IEEE Trans. Circuits Syst. I*, vol. 61, no. 5, pp. 1331–1342, May 2014.

[11] N. Liyanage, L. Bruton, P. Agathoklis, and C. U. S. Edussooriya, "Space-time digital filtering of radio astronomical signals using 3-D cone filters," in *Proc. RFI Mitigation Workshop*, 2010, pp. 1–7.

[12] C. U. S. Edussooriya, L. T. Bruton, P. Agathoklis, and T. K. Gunaratne, "Low-complexity maximally-decimated multirate 3-D spatio-temporal FIR cone and frustum filters," *IEEE Trans. Circuits Syst. I*, vol. 60, no. 7, pp. 1845–1856, Jul. 2013.

[13] C. U. S. Edussooriya, L. T. Bruton, and P. Agathoklis, "A low-complexity 3D spatio-temporal FIR filter for enhancing linear trajectory signals," in *Proc. IEEE Int. Conf. Acoust., Speech, Signal Process.*, 2014, pp. 1165–1169.

[14] D. Dansereau and L. T. Bruton, "A 4-D dual-fan filter bank for depth filtering in light fields," *IEEE Trans. Signal Process.*, vol. 55, no. 2, pp. 542–549, Feb. 2007.

[15] S. U. Premaratne, C. U. S. Edussooriya, C. Wijenayake, L. T. Bruton, and P. Agathoklis, "A 4-D sparse FIR hyperfan filter for volumetric refocusing of light fields by hard thresholding," in *Proc. IEEE Int. Conf. Digital Signal Process.*, 2018, pp. 1–5.

[16] C. U. S. Edussooriya, D. G. Dansereau, L. T. Bruton, and P. Agathoklis, "Five-dimensional depth-velocity filtering for enhancing moving objects in light field videos," *IEEE Trans. Signal Process.*, vol. 63, no. 8, pp. 2151–2163, Apr. 2015.

[17] C. U. S. Edussooriya, L. T. Bruton, and P. Agathoklis, "A novel 5-D depth-velocity filter for enhancing noisy light field videos," *Multidim. Syst. Signal Process.*, vol. 28, no. 1, pp. 353–369, Jan. 2017.

[18] R. Mersereau, W. Mecklenbrauker, and T. Quatieri, "Mcclellan transformations for two-dimensional digital filtering-part I: Design," *IEEE Trans. Circuits Syst.*, vol. 23, no. 7, pp. 405–414, Jul. 1976.

[19] X. Lai, J. Cao, R. Zhao, and Z. Lin, "A relaxed ADMM algorithm for WLS design of linear-phase 2D FIR filters," in *Proc. IEEE Int. Conf. Digital Signal Process.*, Nov. 2018, pp. 1–5.

[20] R. Zhao, X. Lai, and Z. Lin, "Weighted least squares design of 2-D FIR filters using a matrix-based generalized conjugate gradient method," *J. Franklin Institute*, vol. 353, no. 8, pp. 1759–1780, May 2016.

[21] X. Hong, R. Zhao, X. Lai, and J. Cao, "A matrix-based algorithm for the CLS design of centrally symmetric 2-D FIR filters," in *Proc. IEEE Int. Symp. Circuits Syst.*, May 2016, pp. 1230–1233.

[22] X. Hong, X. Lai, and R. Zhao, "A fast design algorithm for elliptic-error and phase-error constrained ls 2-D FIR filters," *Multidim. Syst. Signal Process.*, vol. 27, no. 2, pp. 477–491, Apr. 2016.

[23] ——, "Matrix-based algorithms for constrained least-squares and minimax designs of 2-D linear-phase FIR filters," *IEEE Trans. Signal Process.*, vol. 61, no. 14, pp. 3620–3631, Jul. 2013.

[24] R. Zhao and X. Lai, "Efficient 2-D based algorithms for WLS designs of 2-D FIR filters with arbitrary weighting functions," *Multidim. Syst. Signal Process.*, vol. 24, no. 3, pp. 417–434, Sep. 2013.

[25] W.-S. Lu and T. Hinamoto, "Two-dimensional digital filters with sparse coefficients," *Multidim. Syst. Signal Processing*, vol. 22, no. 1-3, pp. 173–189, Mar. 2011.

[26] X. Lai, "Optimal design of nonlinear-phase FIR filters with prescribed phase error," *IEEE Trans. Signal Process.*, vol. 57, no. 9, pp. 3399–3410, Sep. 2009.

[27] X. Lai and Y. Cheng, "A sequential constrained least-square approach to minimax design of 2-D FIR filters," *IEEE Trans. Circuits Syst. II, Exp. Briefs*, vol. 54, no. 11, pp. 994–998, Nov. 2007.

[28] W.-S. Lu and T. Hinamoto, "A second-order cone programming approach for minimax design of 2-D FIR filters with low group delay," in *Proc. IEEE Int. Symp. Circuits Syst.*, May 2006, pp. 2521–2524.

[29] ——, "A new minimax design for 2D FIR filters with low group delay," in *Proc. IEEE Int. Symp. Circuits Syst.*, May 2005, pp. 2028–2031.

[30] J. L. Aravena and G. Gu, "Weighted least mean square design of 2-D FIR digital filters: the general case," *IEEE Trans. Signal Process.*, vol. 44, no. 10, pp. 2568–2578, Oct. 1996.

[31] S.-C. Pei and J.-J. Shyu, "Design of two-dimensional FIR digital filters by McClellan transformation and least-squares contour mapping," *Signal Process.*, vol. 44, no. 1, pp. 19–26, Jun. 1995.

[32] W.-S. Lu, "A unified approach for the design of 2-D digital filters via semidefinite programming," *IEEE Trans. Circuits Syst. I, Fundam. Theory Appl.*, vol. 49, no. 6, pp. 814–826, Jun. 2002.

[33] T. K. Gunaratne and L. T. Bruton, "Broadband beamforming of bandpass plane waves using 2D FIR trapezoidal filters at baseband," in *Proc. IEEE Asia Pacific Conf. Circuits Syst.*, Dec. 2006, pp. 546–549.

[34] ——, "Adaptive complex-coefficient 2D FIR trapezoidal filters for broadband beamforming in cognitive radio systems," *Circuits Syst. Signal Process.*, vol. 30, no. 3, pp. 587–608, Mar. 2011.

[35] V. Ariyarathna, V. A. Coutinho, S. Pulipati, A. Madanayake, R. T. Wijesekara, C. U. Edussooriya, L. T. Bruton, T. K. Gunaratne, and R. J. Cintra, "Real-time 2-D FIR trapezoidal digital filters for 2.4 GHz aperture receiver applications," in *Proc. Moratuwa Engineering Research Conf.*, 2018, pp. 350–355.

[36] S. Pulipati, V. Ariyarathna, A. Madanayake, R. T. Wijesekara, C. U. Edussooriya, and L. T. Bruton, "A 16-element 2.4-GHz multi-beam array receiver using 2-D spatially-bandpass digital filters," *IEEE Trans. Aerosp. Electron. Syst.*, vol. 55, no. 6, pp. 3029–3038, Dec. 2019.

[37] W. Lawton, "Applications of complex valued wavelet transforms to subband decomposition," *IEEE Trans. Signal Process.*, vol. 41, no. 12, pp. 3566–3568, Dec. 1993.

[38] N. Kingsbury, "Image processing with complex wavelets," *Philosop. Trans. Royal Society of London. Series A: Mathemat., Physical Eng. Sci.*, vol. 357, no. 1760, pp. 2543–2560, Sep. 1999.

[39] ——, "Complex wavelets for shift invariant analysis and filtering of signals," *Appl. Comput. Harmonic Anal.*, vol. 10, no. 3, pp. 234–253, May 2001.

[40] T. Celik and T. Tjahjadi, "Image resolution enhancement using dual-tree complex wavelet transform," *IEEE Geosci. Remote Sens. Lett.*, vol. 7, no. 3, pp. 554–557, Jul. 2010.

[41] W.-P. Zhu, M. O. Ahmad, and M. Swamy, "A least-square design approach for 2D FIR filters with arbitrary frequency response," *IEEE Trans. Circuits Syst. II, Analog Digit. Signal Process.*, vol. 46, no. 8, pp. 1027–1034, Aug. 1999.

[42] J. F. Sturm, "Using SeDuMi 1.02, a MATLAB toolbox for optimization over symmetric cones," *Optim. Methods Softw.*, vol. 11, no. 1-4, pp. 625–653, Mar. 1999.

[43] M. Grant and S. Boyd, "CVX: Matlab software for disciplined convex programming, version 2.1," http://cvxr.com/cvx, Mar. 2014.

[44] ——, "Graph implementations for nonsmooth convex programs," in *Recent Advances in Learning and Control*, ser. Lecture Notes in Control and Information Sciences, V. Blondel, S. Boyd, and H. Kimura, Eds. London: Springer-Verlag, 2008, pp. 95–110, http://stanford.edu/~boyd/graph_dcp.html.

[45] A. Antoniou and W.-S. Lu, *Practical Optimization: Algorithms and Engineering Applications*. NY: Springer, 2007.

[46] H. L. Van Trees, *Optimum Array Processing*. NY: John Wiley & Sons, 2004.

[47] A. Antoniou, *Digital Signal Processing: Signals, Systems and Filters*. NY: McGraw-Hill, 2006.